Practical Performance Model for Bar Buckling

Michael P. Berry[1] and Marc O. Eberhard[2]

Abstract: A practical model has been developed to predict, for a given level of lateral deformation, the likelihood that longitudinal bars in a reinforced concrete column will have begun to buckle. Three relationships linking plastic rotation, drift ratio, and displacement ductility with the onset of bar buckling were derived based on the results of plastic-hinge analysis, moment-curvature analysis, and the expected influence of the confinement reinforcement. These relationships, which account for the effective confinement ratio, axial-load ratio, aspect ratio, and longitudinal bar diameter, were calibrated using observations of bar buckling from cyclic tests of 62 rectangular-reinforced and 42 spiral-reinforced concrete columns. A version of the drift ratio relationship is proposed for earthquake engineering applications. The ratios of the measured displacements at bar buckling to the displacements calculated with the proposed model had a mean of 1.01 and a coefficient of variation of 25% for rectangular-reinforced concrete columns. The corresponding mean and coefficient of variation for spiral-reinforced columns were 0.97 and 24%, respectively.

Introduction

To implement performance-based earthquake engineering, it is necessary to relate deformation demands placed on structural components with the probability of reaching specific levels of damage. The onset of buckling of longitudinal bars in reinforced concrete columns is a key damage state (Fig. 1) because unlike less severe levels of flexural damage, bar buckling requires extensive repairs (Lehman et al. 2001), significantly reduces the structure's functionality (Eberhard 2000), and has clear implications for structural safety. This paper proposes a procedure, intended for earthquake engineering practice, that links lateral deformation demands on reinforced concrete columns with the likelihood that longitudinal bars will have begun to buckle.

Numerous approaches have been proposed to model the instability of longitudinal bars in reinforced concrete columns. Early models used small-deformation, Euler buckling theory to model a reinforcing bar subjected to uniaxial, monotonic compression, restrained laterally by elastic ties (Bresler and Gilbert 1961; Scribner 1986; Papia and Russo 1989). More recent models have considered various details of the complex interaction between the concrete cover, concrete core, confining reinforcement, and longitudinal bars. For example, Pantazopoulou (1998) accounted for the effect of core expansion on tie stiffness and modeled the load

redistribution from the longitudinal bar to the surrounding concrete, as the bar stiffness reduces. Bayrak and Sheikh (2001) considered the pressure exerted directly on the longitudinal reinforcement by the expanding concrete core. Dhakal and Maekawa (2002) estimated the buckling length of the longitudinal reinforcement, accounting for the interaction between concrete cover spalling and bar buckling.

Other studies have considered the effects of cycling on the longitudinal reinforcement. For example, Monti and Nuti (1992); Gomes and Appleton (1997); and Rodriguez et al. (1999) modeled the cyclic, stress-strain response of an isolated reinforcing bar, including the effects of bar buckling (neglecting the influence of the concrete and transverse reinforcement). Moyer and Kowalsky (2001) concluded that models of bar buckling should consider the full deformation history to account for tension strain growth (associated with cyclic inelastic deformations) in the longitudinal reinforcement. Hose (2001) developed models of bar buckling based on the assumption that buckling cannot occur under cyclic loading while the concrete cracks are closed.

These studies, among others, suggest that a comprehensive model of bar buckling in seismic applications would account for the variable length over which bars can buckle, the moment gradient along the column length, the complex, strain-dependent interaction between the concrete cover, concrete core, transverse ties, and longitudinal reinforcement, and the full, cyclic deformation history of the column. Each model provides valuable insight into key factors that contribute to bar instability, but a complete model of bar buckling has not yet been developed.

[1]Graduate Research Assistant, Dept. of Civil and Environmental Engineering, Univ. of Washington, Box 352700, Seattle, WA 98195. E-mail: mpberry@u.washington.edu

[2]Associate Professor, Dept. of Civil and Environmental Engineering, Univ. of Washington, Box 352700, Seattle, WA 98195. E-mail: eberhard@u.washington.edu

Formulation of Deformation Relationships

A practical model, calibrated with numerous observations of bar buckling during lateral, cyclic tests of reinforced concrete columns, is needed for earthquake engineering applications. This section combines plastic-hinge analysis with approximations for the column yield displacement, plastic curvature, buckling strain, and plastic-hinge length to develop three relationships linking

Fig. 1. Typical buckling of longitudinal bar in a spiral-reinforced column

plastic rotation, drift ratio, and displacement ductility with the onset of bar buckling.

Plastic-Hinge Analysis

According to plastic-hinge analysis, the total displacement, Δ, of a reinforced concrete member deformed beyond the yield displacement can be decomposed into two parts, the response up to the yield displacement, Δ_y, and the plastic deformation, Δ_p. The plastic deformation is assumed to result from the rigid-body rotation of the member around the center of a plastic hinge near the base of the column. For simplicity, the curvature in the plastic hinge is assumed to be constant ($\phi_p = \phi - \phi_y$) over an equivalent plastic-hinge length, L_p, as shown in Fig. 2. The plastic rotation, θ_p, can then be expressed as $\phi_p L_p$, and the total tip deflection is

$$\Delta = \Delta_y + \theta_p(L - L_p/2) = \Delta_y + (\phi_p L_p)(L - L_p/2) \quad (1)$$

where L=distance from the column base to the point of contraflexure.
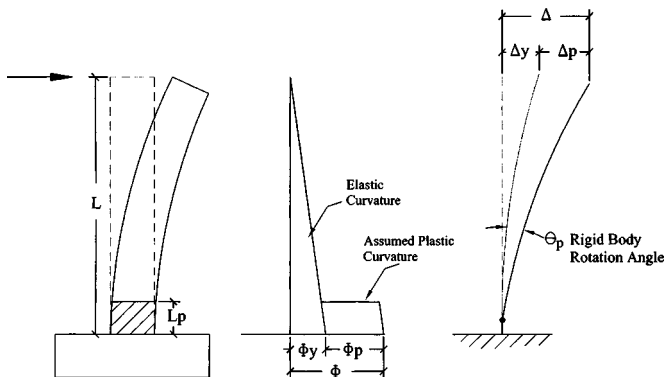

Fig. 2. Plastic-hinge analysis

If $L_p/2 \ll L$ and longitudinal bar buckling is assumed to occur after column yielding, the displacement at the onset of bar buckling can be expressed as

$$\Delta_{bb} = \Delta_y + \phi_{p\_bb}L_pL \quad (2)$$

where ϕ_{p_bb}=plastic curvature at the onset of bar buckling. The following sections present approximations for three terms in Eq. (2), namely Δ_y, ϕ_{p_bb}, and L_p.

Column Yield Displacement

Priestley et al. (1996) proposed an approximation for the yield curvature of a reinforced concrete column, based on the column depth and the yield strain of the tension reinforcement (ε_y).

$$\phi_y \cong \lambda \frac{\varepsilon_y}{D} \quad (3)$$

where $\lambda = 2.45$ for spiral-reinforced columns and 2.14 for rectangular-reinforced columns. Assuming that the moment-curvature relationship is linear up to the column yield point, the yield displacement can be approximated as

$$\Delta_y \cong \frac{\phi_y L^2}{3} \cong \frac{\lambda}{3}\varepsilon_y\frac{L^2}{D} = \frac{\lambda}{3E_s}f_y\frac{L^2}{D} \quad (4)$$

where E_s and f_y=elastic modulus and yield stress of the longitudinal reinforcement, respectively. For simplicity, Eq. (4) neglects the effects of shear deformation and strain penetration.

Plastic Curvature

Based on axial equilibrium requirements for a reinforced concrete cross section, Berry (2003) showed that the location of the neutral axis depends mainly on the level of axial load, and to a lesser extent, on the amount of longitudinal reinforcement. Berry (2003) found that the normalized plastic curvature ($\phi_{p\_norm} = \phi_{p\_n}D/\varepsilon_n$) at a given extreme compression fiber strain (ε_n) can be approximated with the following equation:

$$\frac{\phi_{p\_n}D}{\varepsilon_n} = \frac{G_0}{1 + G_1\dfrac{P}{A_g f'_c}} \quad (5)$$

where D=column depth; P=axial load; A_g=gross area of the cross section; and f'_c=compressive strength of the concrete. G_0 and G_1=parameters that depend on the level of strain. For example, at a maximum strain of $\varepsilon_n = 0.004$, G_0 and G_1 can be taken as 5.3 and 9.4, respectively.

The normalized plastic curvatures (computed with moment-curvature analysis) for a compressive strain of $\varepsilon_n = 0.004$ are compared with curvatures calculated with Eq. (5) in Fig. 3 for 288 flexure-dominant columns (www.ce.washington.edu/~peeral). The columns were classified as flexure-dominant as defined in Berry and Eberhard (2004). The ratios of the plastic curvatures calculated with moment-curvature analysis to the plastic curvatures calculated with Eq. (5) had a mean of 1.0 with a coefficient of variation of 18%. According to Berry (2003) this equation can also be used to approximate the relationship between the strain at the onset of bar buckling (ε_{bb}) with the curvature at the onset of bar buckling (ϕ_{p_bb}).

The strain ε_{bb} is influenced by the transverse reinforcement, which confines the concrete core and tends to restrain the longitudinal bars from buckling. A common measurement of the effectiveness of the transverse reinforcement is the effective confine-
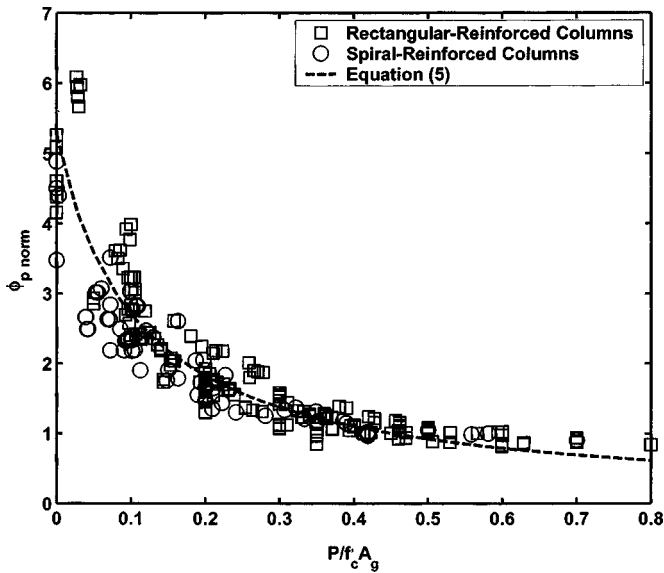
Fig. 3. Evaluation of approximation for plastic curvature

Fig. 4. Definition of displacement preceding the onset of bar buckling

ment ratio, defined as $\rho_{eff} = \rho_s f_{ys}/f_c'$, where ρ_s=volumetric transverse reinforcement ratio; f_{ys}=yield stress of transverse reinforcement; and f_c'=concrete compressive strength. For example, Saatcioglu and Razvi (1994) found that axial strain ductility capacity was approximately constant for a given effective confinement ratio.

For development of the proposed deformation relationships, the buckling strain is assumed to vary linearly as a function of the effective confinement ratio, as follows

$$\varepsilon_{bb} = \chi_0(1 + \chi_1\rho_{eff}) \qquad (6)$$

where χ_0 and χ_1=constants. The parameter χ_1 is expected to be larger for spiral-reinforced columns because spiral reinforcement is more effective than rectangular reinforcement at confining the core and longitudinal reinforcement. This relationship is similar to the relationship that Pantazopoulou (1998) proposed for 20% reduction in flexural strength. In this formulation the transverse confinement spacing, s, is taken into account by its effect on ρ_s.

By substituting Eq. (6) into Eq. (5) and combining constants, the plastic curvature at the onset of bar buckling can be approximated with

$$\phi_{p\_bb} \cong \frac{\eta_0}{D}\left(\frac{1 + \eta_1\rho_{eff}}{1 + \eta_2\dfrac{P}{A_g f_c'}}\right) \qquad (7)$$

where η_0, η_1, and η_2=constants.

Plastic-Hinge Length

Numerous models have been proposed to estimate the plastic-hinge length of structural members (Sawyer 1964; Corley 1966; Mattock 1967; Priestley and Park 1987; Priestley et al. 1996). In many of these models, the expression for the plastic-hinge length is proportional to the column length, L, column depth, D, and the longitudinal reinforcement properties, as in the following equation:

$$L_p = \alpha L + \beta D + \xi f_y d_b \qquad (8)$$

where d_b=bar diameter of the tension reinforcement. For example, in the equation developed by Mattock (1967), α
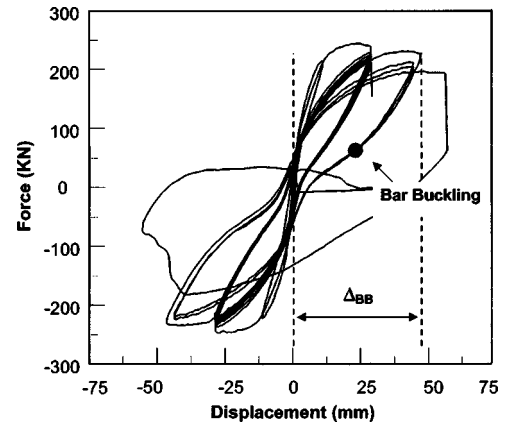
=1/20, β=1/2, and ξ=0. In the Priestley et al. (1996) model, α=0.08, β=0, and ξ=0.022 (f_y in MPa), with an upper limit on L_p of $0.044f_y d_b$.

The deformation relationships derived in this section adopt the general form of Eq. (8), in which α, β, and ξ are unknown constants. The column length is included in Eq. (8) to account for the moment gradient along the length of the cantilever, and the column depth is included to account for the influence of shear on the size of the plastic region. The longitudinal bar properties are included to account for additional rotation at the plastic-hinge resulting from strain penetration of the longitudinal reinforcement into the supporting element.

Deformations at Bar Buckling

Three commonly used engineering demand parameters (plastic rotation, drift ratio, and displacement ductility) can be approximated by combining plastic-hinge analysis with the approximations of yield displacement, plastic curvature, and plastic-hinge length. By substituting the approximations for plastic curvature (7) and plastic-hinge length (8) into the definition of plastic rotation ($\theta_p = \phi_p L_p$), the plastic rotation at the onset of bar buckling can be expressed as

$$\theta_{p\_bb} = C_0(1 + C_1\rho_{eff})\left(1 + C_2\frac{P}{A_g f_c'}\right)^{-1}\left(1 + C_3\frac{L}{D} + C_4\frac{f_y d_b}{D}\right) \qquad (9)$$

The five constants in Eq. (9) ($C_0,\ldots,C_4$) are combinations of the constants included in Eqs. (5) and (7). By substituting Eqs. (4) and (9) into Eq. (2), and dividing by the column length, the drift ratio at the onset of bar buckling can be expressed as follows:

$$\frac{\Delta_{bb}}{L} = \frac{\lambda}{3E_s}f_y\frac{L}{D} + C_0(1 + C_1\rho_{eff})\left(1 + C_2\frac{P}{A_g f_c'}\right)^{-1}$$
$$\times\left(1 + C_3\frac{L}{D} + C_4\frac{f_y d_b}{D}\right) \qquad (10)$$

If Eq. (10) is divided by the yield displacement and multiplied by the column length, the displacement ductility at the onset of bar buckling can be expressed as

Table 1. Maximum Deformations Preceding Bar Buckling in Rectangular-Reinforced Columns

Reference	Designation	Δ_{bb} (mm)	θ_{p_bb}	Δ_{bb}/L (%)	Δ_{bb}/Δ_y	L/D	ρ_{eff}	P/f_cA_g	d_b/D	f_y (MPa)
Ghee et al. (1981)	No. 3	50.0	0.028	3.1	5.2	4.0	0.39	0.38	0.04	427
Ghee et al. (1981)	No. 4	58.0	0.031	3.6	4.8	4.0	0.25	0.21	0.04	427
Soesianawati et al. (1986)	No. 1	78.4	0.047	4.9	7.6	4.0	0.07	0.10	0.04	446
Soesianawati et al. (1986)	No. 2	68.4	0.041	4.3	7.5	4.0	0.10	0.30	0.04	446
Soesianawati et al. (1986)	No. 3	44.9	0.025	2.8	5.1	4.0	0.07	0.30	0.04	446
Soesianawati et al. (1986)	No. 4	41.0	0.024	2.8	4.6	4.0	0.04	0.30	0.04	446
Zahn et al. (1986)	No. 7	71.0	0.044	4.7	6.3	4.0	0.27	0.22	0.04	440
Zahn et al. (1986)	No. 8	50.0	0.037	4.0	6.3	4.0	0.24	0.39	0.04	440
Tanaka and Park (1990)	No. 1	120.0	0.074	7.5	8.7	4.0	0.33	0.20	0.05	474
Tanaka and Park (1990)	No. 2	87.2	0.052	5.5	6.7	4.0	0.33	0.20	0.05	474
Tanaka and Park (1990)	No. 3	59.0	0.033	3.7	5.2	4.0	0.33	0.20	0.05	474
Tanaka and Park (1990)	No. 4	80.0	0.047	5.0	6.5	4.0	0.33	0.20	0.05	474
Tanaka and Park (1990)	No. 5	73.8	0.041	4.5	5.4	3.0	0.17	0.10	0.04	511
Tanaka and Park (1990)	No. 6	67.2	0.038	4.1	5.6	3.0	0.17	0.10	0.04	511
Tanaka and Park (1990)	No. 7	82.4	0.049	5.0	8.5	3.0	0.21	0.30	0.04	511
Tanaka and Park (1990)	No. 8	78.0	0.047	4.7	9.3	3.0	0.21	0.30	0.04	511
Park and Paulay (1990)	No. 9	84.0	0.046	4.7	7.8	3.0	0.31	0.10	0.04	432
Atalay and Penzien (1975)	6S1	40.7	0.014	2.4	2.1	5.5	0.11	0.18	0.07	429
Wehbe et al. (1998)	A1	122.0	0.046	5.2	5.2	3.8	0.10	0.10	0.03	448
Wehbe et al. (1998)	A2	102.0	0.037	4.4	4.6	3.8	0.10	0.24	0.03	448
Wehbe et al. (1998)	B2	128.0	0.047	5.5	4.8	3.8	0.13	0.23	0.03	448
Xiao and Martirossyan (1998)	HC48L19T10-0.1P	47.0	0.107	9.3	7.6	2.0	0.23	0.10	0.08	510
Xiao and Martirossyan (1998)	HC48L19T10-0.2P	40.0	0.091	7.9	7.6	2.0	0.23	0.20	0.08	510
Xiao and Martirossyan (1998)	HC48L16T10-0.1P	37.0	0.080	7.3	7.1	2.0	0.20	0.10	0.06	510
Xiao and Martirossyan (1998)	HC48L16T10-0.2P	35.0	0.072	6.9	5.6	2.0	0.20	0.19	0.06	510
Bayrak and Sheikh (1996)	ES-1HT	48.5	0.018	2.5	5.6	6.0	0.18	0.50	0.06	454
Bayrak and Sheikh (1996)	AS-2HT	95.1	0.039	5.0	9.5	6.0	0.20	0.36	0.06	454
Bayrak and Sheikh (1996)	AS-3HT	62.6	0.025	3.3	7.4	6.0	0.20	0.50	0.06	454
Bayrak and Sheikh (1996)	AS-4HT	78.5	0.033	4.4	6.6	6.0	0.29	0.50	0.06	454
Bayrak and Sheikh (1996)	AS-6HT	73.3	0.028	3.8	5.6	6.0	0.27	0.46	0.06	454
Bayrak and Sheikh (1996)	AS-7HT	31.0	0.014	2.3	3.3	6.0	0.13	0.45	0.06	454
Bayrak and Sheikh (1996)	ES-8HT	26.6	0.014	2.0	4.4	6.0	0.17	0.47	0.06	454
Saatcioglu and Grira (1999)	BG2	82.3	0.049	5.0	8.5	4.7	0.49	0.43	0.06	456
Saatcioglu and Grira (1999)	BG4	65.8	0.037	4.0	6.0	4.7	0.24	0.46	0.06	456
Saatcioglu and Grira (1999)	BG5	115.2	0.068	7.0	8.4	4.7	0.49	0.46	0.06	456
Saatcioglu and Grira (1999)	BG8	115.2	0.064	7.0	5.6	4.7	0.24	0.23	0.06	456
Saatcioglu and Grira (1999)	BG9	65.8	0.036	4.0	5.3	4.7	0.24	0.46	0.05	428
Thomsen and Wallace (1994)	A3	23.9	0.056	5.4	9.2	3.9	0.13	0.20	0.06	517
Thomsen and Wallace (1994)	D1	47.8	0.047	4.9	6.3	3.9	0.21	0.20	0.06	476
Thomsen and Wallace (1994)	D2	35.8	0.046	4.9	5.7	3.9	0.15	0.20	0.06	476
Thomsen and Wallace (1994)	D3	35.8	0.045	4.9	5.2	3.9	0.16	0.20	0.06	476
Xiao and Yun (2002)	No. FHC1-0.2	142.2	0.082	8.0	9.6	3.5	0.19	0.20	0.07	375
Xiao and Yun (2002)	No. FHC2-0.34	71.1	0.038	4.0	6.4	3.5	0.19	0.33	0.07	375
Xiao and Yun (2002)	No. FHC3-0.22	106.7	0.060	6.0	7.7	3.5	0.18	0.22	0.07	375
Xiao and Yun (2002)	No. FHC4-0.33	71.1	0.038	4.0	6.3	3.5	0.18	0.32	0.07	375
Xiao and Yun (2002)	No. FHC5-0.2	106.7	0.060	6.0	7.6	3.5	0.12	0.20	0.07	427
Xiao and Yun (2002)	No. FHC6-0.2	106.7	0.059	6.0	6.7	3.5	0.15	0.20	0.07	427
Bayrak (1998)	RS- 9HT	128.6	0.051	6.7	7.6	5.3	0.25	0.34	0.06	446
Bayrak (1998)	RS-10HT	85.9	0.034	4.5	7.0	5.3	0.25	0.50	0.06	446
Bayrak (1998)	RS-12HT	82.9	0.031	4.3	6.0	5.3	0.13	0.34	0.06	446
Bayrak (1998)	RS-13HT	89.8	0.034	4.7	6.1	5.3	0.16	0.35	0.06	440
Bayrak (1998)	RS-14HT	62.6	0.016	3.2	2.4	5.3	0.16	0.46	0.06	440
Bayrak (1998)	RS-15HT	117.9	0.041	6.0	4.5	5.3	0.22	0.36	0.06	474
Bayrak (1998)	RS-16HT	79.8	0.026	4.1	3.7	5.3	0.15	0.37	0.06	474
Bayrak (1998)	RS-17HT	106.7	0.036	5.4	4.0	5.3	0.33	0.34	0.06	474

Table 1. (*Continued.*)

Reference	Designation	Δ_{bb} (mm)	θ_{p_bb}	Δ_{bb}/L (%)	Δ_{bb}/Δ_y	L/D	ρ_{eff}	$P/f_c A_g$	d_b/D	f_y (MPa)
Bayrak (1998)	RS-18HT	64.5	0.022	3.3	4.2	5.3	0.33	0.50	0.06	474
Bayrak (1998)	RS-19HT	121.7	0.049	6.3	8.1	5.3	0.64	0.53	0.06	474
Bayrak (1998)	RS-20HT	66.0	0.021	3.4	3.4	5.3	0.34	0.34	0.06	474
Bayrak (1998)	WRS-21HT	67.2	0.018	3.4	2.6	7.4	0.19	0.47	0.08	474
Bayrak (1998)	WRS-22HT	126.9	0.044	6.5	4.3	7.4	0.19	0.31	0.08	474
Bayrak (1998)	WRS-23HT	122.5	0.042	6.3	4.3	7.4	0.25	0.33	0.08	474
Bayrak (1998)	WRS-24HT	87.0	0.029	4.5	3.7	7.4	0.25	0.50	0.08	511
Statistics	Mean	76.8	0.043	4.8	6.0	4.5	0.22	0.30	0.06	458
	Standard deviation	30.0	0.019	1.5	1.8	1.3	0.11	0.13	0.01	34
	COV	0.39	0.44	0.33	0.30	0.29	0.48	0.42	0.24	0.07
	Minimum	23.9	0.014	2.0	2.1	2.0	0.04	0.10	0.03	375
	Maximum	142.2	0.107	9.3	9.6	7.4	0.64	0.53	0.08	517

$$\frac{\Delta_{bb}}{\Delta_y} = 1 + \frac{3E_s}{\lambda f_y} C_0 (1 + C_1 \rho_{\text{eff}}) \left(1 + C_2 \frac{P}{A_g f'_c}\right)^{-1}$$
$$\times \left(\frac{1}{L/D} + C_3 + C_4 \frac{1}{L/D} \frac{f_y d_b}{D}\right) \qquad (11)$$

The constants in Eqs. (9), (10), and (11) can be evaluated from experimental observations of bar buckling.

Column Performance Database

To calibrate models of column behavior, the results of 467 cyclic, lateral-load tests of reinforced concrete columns were assembled in a database, which is available on the World Wide Web at www.ce.washington.edu/~peera1 and http://peer.berkeley.edu/. For each test, the database provides the column geometry, material properties, reinforcement details, loading configuration, a reference, and test results. The test results provided include the digital force-displacement history for the column (or in a few cases, the force-displacement envelope), as well as the maximum column deflection imposed before reaching various damage states, including the onset of bar buckling, Δ_{bb}. The definition of Δ_{bb} is illustrated in Fig. 4.

To calibrate Eqs. (9), (10), and (11), the tests were screened according to the following criteria: (1) the column needed to be flexure-critical, as defined by Berry and Eberhard (2004); (2) the aspect ratio had to exceed 1.9; (3) the longitudinal reinforcement had to be continuous (unspliced); and (4) the displacement preceding bar buckling had to be documented. For the 62 rectangular-reinforced and 42 spiral-reinforced column tests that met the screening criteria, Tables 1 and 2 provide values of the maximum deformations preceding the onset of bar buckling, as well as key column properties. The mean values of the plastic rotations, drift ratios, and displacement ductilities for the rectangular-reinforced columns were 0.043, 4.8%, and 6.0, respectively. The corresponding mean values for the spiral-reinforced columns were 0.060, 6.6%, and 6.8, respectively.

The experimental data support the general form of Eqs. (9), (10), and (11). For example, Fig. 5 (rectangular-reinforced col-

umns) and Fig. 6 (spiral-reinforced columns) show the variation of the drift ratio at the onset of bar buckling as a function of key column properties. To isolate the effect of each property, the database was organized into families, in which all columns in a family had similar properties except for the property being studied. These families are connected with lines in Figs. 5 and 6. It should be noted that the families do not take into consideration variations in the displacement history imposed on each column. As expected from Eq. (10), the drift ratio at the onset of longitudinal bar buckling decreases with an increase in $P/A_g f'_c$, and increases with an increase in ρ_{eff}, $f_y d_b/D$, and L/D.

Calibration of Column Deformation Relationships

The column database was used to calibrate the column deformation relationships. Specifically, the values of the unknown constants $(C_0, \dots, C_4)$ in Eqs. (9), (10), and (11) were determined such that (1) the ratios of the measured damage displacements (from the column database) to the calculated damage displacements had a mean value equal to 1.0; and (2) the coefficient of variation (COV) of the ratios was minimized. The resulting values of the constants for each measure of column deformation are provided in Table 3, along with statistical measures of the accuracy of the resulting equations. The objective functions [(9)–(11)] used in the regression analyses contained a number of local minima with similar magnitudes. As a result one cannot directly compare the values of $C_0, \dots, C_4$ among the three equations and two column types. The COVs of the ratios of measured displacements to calculated displacements are similar for plastic rotation, drift ratio, and displacement ductility, ranging from 20 to 29%, depending on the particular measure of deformation, and depending on whether the columns were reinforced with spirals or rectangular ties.

Berry and Eberhard (2003) showed that the accuracies of the estimates of Δ_{bb} calculated with Eqs. (9), (10), and (11) can be increased slightly by using more complex models of bar buckling. However, the increases in accuracy did not justify the added complexity. Some of the scatter in the values of $\Delta_{bb}/\Delta_{bb\ \text{calc}}$ likely arises from the influence of repeated deformation cycling

Table 2. Maximum Deformations Preceding Bar Buckling in Spiral-Reinforced Columns

Reference	Designation	Δ_{bb} (mm)	θ_{p_bb}	Δ_{bb}/L (%)	Δ_{bb}/Δ_y	L/D	ρ_{eff}	P/f_cA_g	d_b/D	f_y (MPa)
Davey (1975)	No. 1	96.8	0.03	4.8	3.7	5.5	0.04	0.06	0.04	373
Davey (1975)	No. 2	70.5	0.04	3.5	8.0	3.5	0.04	0.05	0.04	371
Davey (1975)	No. 3	157.4	0.04	7.9	3.8	6.5	0.04	0.05	0.04	373
Ghee et al. (1981)	No. 1	60.0	0.03	3.8	6.9	4.0	0.09	0.20	0.04	308
Ghee et al. (1981)	No. 2	50.0	0.03	3.1	5.8	4.0	0.15	0.56	0.04	308
Zahn et al. (1986)	No. 5	45.6	0.02	2.9	4.8	4.0	0.09	0.13	0.04	337
Watson (1989)	No 11	36.3	0.02	2.3	5.9	4.0	0.13	0.70	0.04	474
Wong et al. (1990)	No. 1	41.4	0.05	5.2	7.1	2.0	0.11	0.19	0.04	423
Wong et al. (1990)	No. 3	28.8	0.04	3.6	6.8	2.0	0.11	0.39	0.04	475
Stone and Cheok (1989)	Flexure	538.0	0.05	5.9	4.9	6.0	0.09	0.07	0.03	475
Stone and Cheok (1989)	Shear	285.0	0.06	6.2	6.9	3.0	0.19	0.07	0.03	475
Cheok and Stone (1986)	N1	82.5	0.11	11.0	11.2	3.0	0.26	0.10	0.03	446
Cheok and Stone (1986)	N2	46.6	0.06	6.2	7.6	3.0	0.27	0.21	0.03	446
Cheok and Stone (1986)	N3	110.6	0.07	7.4	6.9	6.0	0.13	0.10	0.03	446
Cheok and Stone (1986)	N4	53.3	0.07	7.1	11.0	3.0	0.25	0.10	0.03	446
Cheok and Stone (1986)	N5	52.2	0.07	7.0	8.3	3.0	0.26	0.20	0.03	446
Cheok and Stone (1986)	N6	71.5	0.04	4.8	5.0	6.0	0.14	0.10	0.03	446
Kunnath et al. (1997)	No. A2	64.5	0.04	4.7	4.7	4.5	0.14	0.09	0.03	448
Kunnath et al. (1997)	No. A7	80.0	0.05	5.8	7.2	4.5	0.13	0.09	0.03	448
Kunnath et al. (1997)	No. A8	80.0	0.05	5.8	5.2	4.5	0.13	0.09	0.03	448
Kunnath et al. (1997)	No. A9	63.0	0.04	4.6	5.3	4.5	0.13	0.09	0.03	448
Kunnath et al. (1997)	No. A10	90.7	0.06	6.6	7.5	4.5	0.15	0.10	0.03	448
Kunnath et al. (1997)	No. A12	81.0	0.05	5.9	7.2	4.5	0.15	0.10	0.03	448
Hose et al. (1997)	No. SRPH1	320.0	0.08	8.7	8.1	6.0	0.09	0.15	0.04	455
Vu et al. (1998)	No. NH3	50.0	0.06	5.5	8.3	2.0	0.12	0.15	0.03	428
Kowalsky et al. (1999)	No. FL3	340.0	0.08	9.3	5.7	8.0	0.11	0.28	0.03	477
Lehman and Moehle (2000)	No. 415	129.0	0.05	5.3	7.4	4.0	0.14	0.07	0.03	462
Lehman and Moehle (2000)	No. 815	445.0	0.08	9.1	6.9	8.0	0.14	0.07	0.03	462
Lehman and Moehle (2000)	No. 1015	635.0	0.09	10.4	5.8	10.0	0.14	0.07	0.03	462
Lehman and Moehle (2000)	No. 407	127.0	0.05	5.2	9.7	4.0	0.14	0.07	0.03	462
Lehman and Moehle (2000)	No. 430	178.0	0.07	7.3	6.8	4.0	0.14	0.07	0.03	462
Calderone et al. (2000)	No. 328	133.0	0.07	7.3	9.0	3.0	0.16	0.09	0.03	441
Calderone et al. (2000)	No. 828	600.0	0.11	12.3	7.3	8.0	0.16	0.09	0.03	441
Calderone et al. (2000)	No. 1028	889.0	0.13	14.6	9.4	10.0	0.16	0.09	0.03	441
Saatcioglu and Baingo (1999)	No. RC6	68.4	0.04	4.2	6.4	6.6	0.08	0.42	0.06	419
Nelson (2000)	Col2	56.6	0.03	3.7	6.3	3.0	0.01	0.11	0.03	455
Henry and Mahin (1999)	No. 415p	127.0	0.04	5.2	5.0	4.0	0.11	0.12	0.03	462
Henry and Mahin (1999)	No. 415s	127.0	0.05	5.2	5.4	4.0	0.06	0.06	0.03	462
Moyer and Kowalsky (2002)	No. 1	149.9	0.05	6.1	4.0	5.3	0.12	0.04	0.04	565
Moyer and Kowalsky (2002)	No. 2	261.6	0.10	10.7	6.4	5.3	0.12	0.04	0.04	565
Moyer and Kowalsky (2002)	No. 3	261.9	0.10	10.7	7.2	5.3	0.13	0.04	0.04	565
Moyer and Kowalsky (2002)	No. 4	297.2	0.12	12.2	7.4	5.3	0.12	0.04	0.04	565
Statistics	Mean	178.1	0.060	6.6	6.8	4.8	0.13	0.14	0.03	448
	Standard deviation	191.2	0.027	2.8	1.7	1.9	0.06	0.14	0.01	57
	COV	1.07	0.45	0.43	0.26	0.40	0.43	0.98	0.22	0.13
	Minimum	28.82	0.021	2.3	3.7	2.0	0.01	0.04	0.03	308
	Maximum	889.00	0.134	14.6	11.2	10.0	0.27	0.70	0.06	565

(Kunnath et al. 1997; Ranf et al. 2003). In addition, the identification of the onset of bar buckling is subjective and may vary among observers. The typical practice of imposing a series of successively increasing cycles to discrete levels of deformation leads to further scatter. For example, consider Fig. 4, in which bar buckling is identified to occur after an imposed displacement of 50 mm. The bars did not buckle at a displacement of 25 mm, but it is impossible to know whether the bars would have buckled if a displacement between 25 and 50 mm had been imposed on the column.

Practical Implementation

The accuracies of the deformation relationships based on plastic rotation (9), drift ratio (10), and displacement ductility (11) were
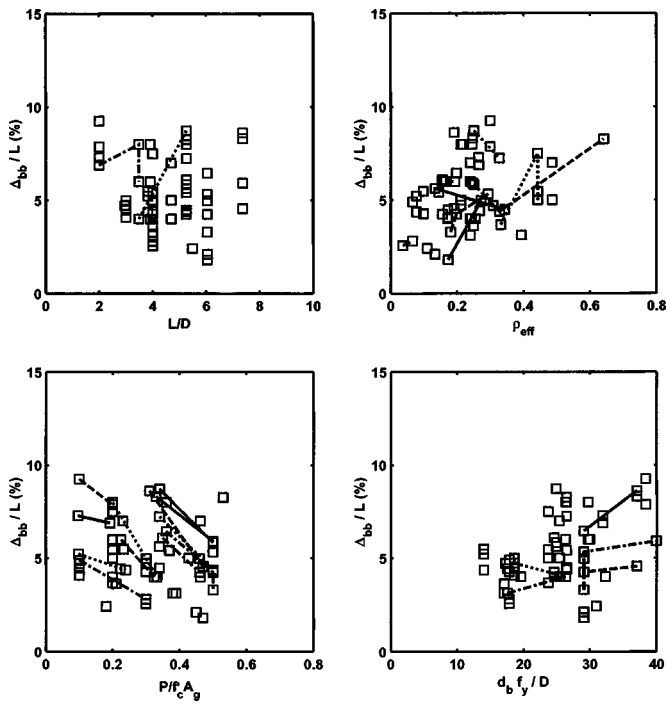
Fig. 5. Drift ratio at bar buckling for rectangular-reinforced columns

Fig. 6. Drift ratio at bar buckling for spiral-reinforced columns

similar. Since it is easiest to compute the drift ratio (drift ratio can be calculated without estimating the yield displacement, an estimate that introduces further error) practical recommendations were developed based on the drift ratio relationship. For practical implementation, the following relationship, a simpler version of Eq. (10), is proposed to approximate the drift ratio at the onset of bar buckling in reinforced concrete columns.

$$\frac{\Delta_{bb\_calc}}{L}(\%) = 3.25\left(1 + k_{e\_bb}\rho_{\text{eff}}\frac{d_b}{D}\right)\left(1 - \frac{P}{A_g f'_c}\right)\left(1 + \frac{L}{10D}\right)$$
(12)

where $k_{e\ bb}=40$ for rectangular-reinforced columns and 150 for spiral-reinforced columns. The form of Eq. (12) was obtained from Eq. (10) by combining the transverse and longitudinal reinforcement properties controlling the onset of bar buckling into a new parameter, $\rho_{\text{eff}}d_b/D$, fixing the exponents of Eq. (10) to 1.0, and forcing the coefficients of Eq. (10) to be the same for spiral and rectangular-reinforced columns, except for the coefficient multiplying ρ_{eff}.

Berry (2003) showed that the accuracy of Eq. (12) does not vary significantly with the axial-load ratio, aspect ratio, effective confinement ratio, and longitudinal reinforcement ratio. In addi-
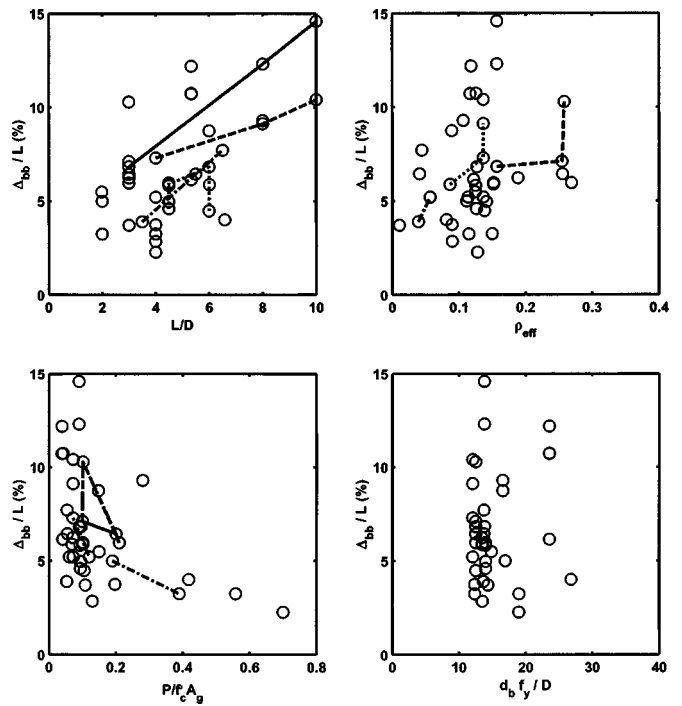
tion, the accuracy did not vary consistently with the ratio of the confinement spacing to the bar diameter (s/d_b). Although the data available did not document the buckling mode, this slenderness ratio would be expected to be significant for bar buckling between two adjacent hoops or spirals. Since little data are available for large values of s/d_b, $k_{e\ bb}$ should be taken as 0.0 for columns with s/d_b exceeding 6. The accuracy of Eq. (12) with the limit on s/d_b is similar to that of Eq. (10). The mean and coefficient of variation for $\Delta_{bb}/\Delta_{bb\ calc}$ calculated using Eq. (12) were 1.01 and 25% for rectangular-reinforced columns, and 0.97 and 24% for spiral-reinforced columns.

The form of Eq. (12) is consistent with the expected behavior of reinforced concrete columns. The effective confinement ratio, ρ_{eff}, accounts for the restraint against bar buckling that the transverse reinforcement provides. The values of $k_{e\ bb}$ for spiral- and rectangular-reinforced columns differ because spiral reinforcement is more effective than rectangular ties at confining the core and the longitudinal reinforcement. The normalized bar diameter, d_b/D, reflects the increased stability of larger bars and the influence of strain penetration into the column base. The axial-load ratio term is consistent with the results of moment-curvature analysis, which indicate that, for the same maximum compression strain, columns with higher axial loads have lower curvatures.

Table 3. Results of Regression Analyses

Column deformation	Column type	Coefficients					Statistics of $\Delta_{bb}/\Delta_{\text{calc}}$			
		C0	C1	C2	C3	C4	Minimum	Maximum	Mean	Coefficient of variation
θ_{p_bb} (9)	Rectangular-reinforced	0.019	1.650	1.797	0.012	0.072	0.40	1.61	1.00	0.25
	Spiral-reinforced	0.006	7.190	3.129	0.651	0.227	0.60	1.39	1.00	0.20
Δ_{bb}/L (10)	Rectangular-reinforced	1.472	1.326	1.875	0.288	0.078	0.37	1.63	1.00	0.26
	Spiral-reinforced	0.309	5.740	2.810	1.764	0.469	0.58	1.46	1.00	0.22
Δ_{bb}/Δ_y (11)	Rectangular-reinforced	0.014	1.277	0.273	0.237	−0.001	0.43	1.83	1.00	0.29
	Spiral-reinforced	0.005	4.534	1.302	1.010	0.032	0.60	1.50	1.00	0.22

(a)

(b)

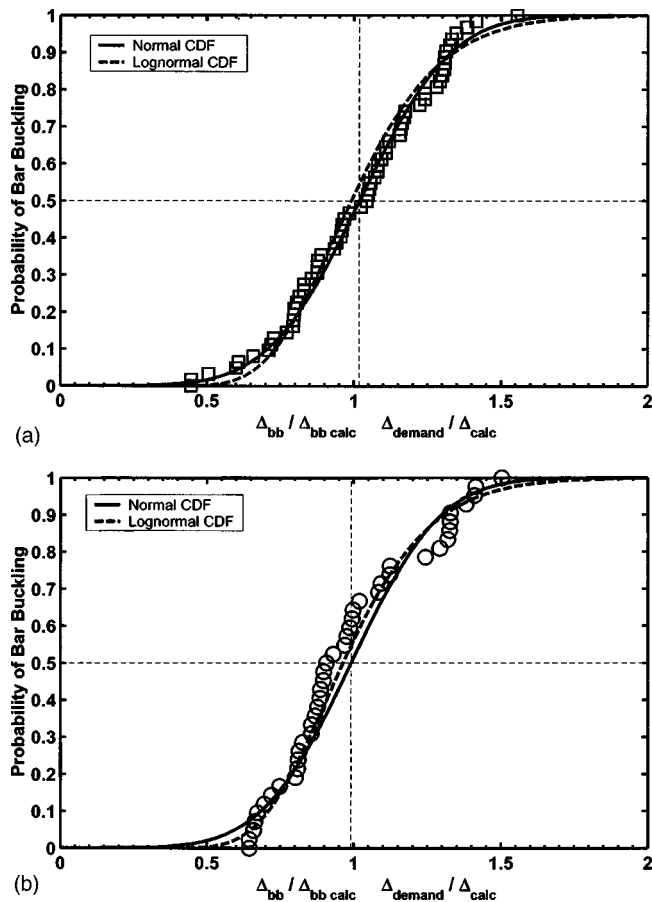**Fig. 7.** Fragility curves for onset of bar buckling: (a) rectangular reinforced columns and (b) spiral-reinforced columns

Fig. 8. Implications for evaluation of spiral-reinforced columns: ($P/Agf'c=30\%$, $L/D=4$, $D/db=14$)

ing drift ratio and decreases with increasing amount of confinement reinforcement. The figure was generated (using a normal CDF) for spiral-reinforced columns with an axial-load ratio of 30%, an aspect ratio of 4, and $d_b/D=1/14$. Similar plots can be generated for other column types and other models of statistical distribution (e.g., lognormal).

To design new columns, the column deformation demand, aspect ratio, and axial-load ratio are known and the acceptable probability of bar buckling is specified. For a specified probability of bar buckling, the target $\Delta_{\text{demand}}/\Delta_{bb\text{ calc}}$ can be estimated from the fragility curves. Rearranging Eq. (12), the transverse reinforcement can be proportioned as follows:

The span-to-depth ratio, L/D, affects the drift ratio at bar buckling by increasing the normalized yield displacement and the length of the plastic hinge, as shown in Eq. (10).

To estimate the likelihood of bar buckling, Eq. (12) can be combined with fragility curves, such as those shown in Fig. 7. This figure shows the cumulative probability of bar buckling as a function of $\Delta_{bb}/\Delta_{bb\text{ calc}}$ for the database, as well as the corresponding normal cumulative distribution functions (CDF) and the lognormal CDF. The normal CDF approximates the column data better than the lognormal CDF. However, the normal distribution may cause problems if applied at extremely low levels of probability because it yields negative values of $\Delta_{bb}/\Delta_{bb\text{ calc}}$, which have no meaningful physical interpretation.

To apply Eq. (12) in practice, it is necessary to assume that the database is representative of the general population of rectangular- and spiral-reinforced columns. To evaluate existing columns, the displacement demand, Δ_{demand}, is estimated based on an analysis of the full structure. The estimated displacement at bar buckling, $\Delta_{bb\text{ calc}}$, is then calculated with Eq. (12) based on the known column properties. The probability that a longitudinal bar will have buckled at or before that displacement demand is then evaluated from the appropriate fragility curve (CDF) shown in Fig. 7. For example, if $\Delta_{\text{demand}}/\Delta_{bb\text{ calc}}$ is equal to 2/3 for a spiral-reinforced concrete column, the probability that a bar will have begun to buckle at or before the displacement demand is 10%.

The implications of applying the proposed evaluation procedure to reinforced concrete columns can be seen in Fig. 8, which shows that the probability of bar buckling increases with increas-
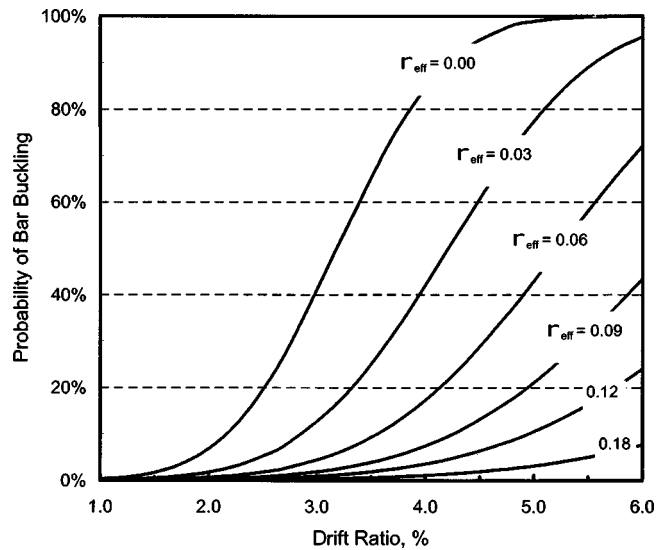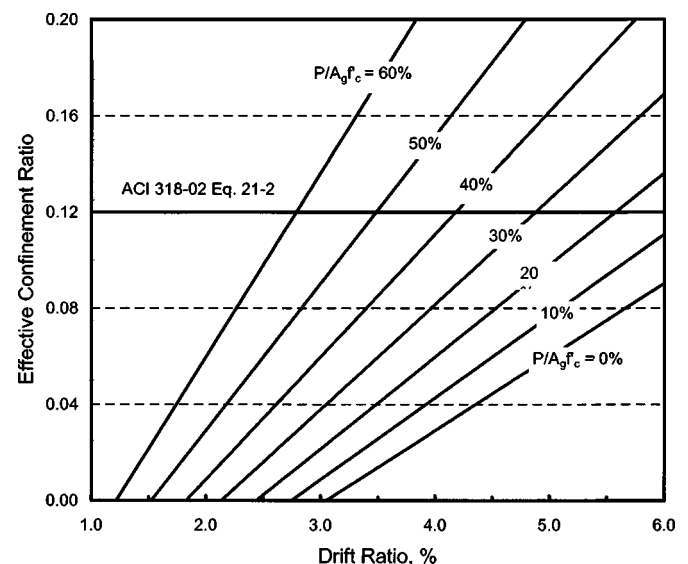

Fig. 9. Implications for design of spiral-reinforced columns: 10% probability of onset of buckling ($L/D=4$, $D/db=14$)

$$\rho_{\text{eff}} = \left(\frac{D}{k_{e\_bb}d_b}\right)\left(\frac{\dfrac{\dfrac{\Delta_{\text{demand}}}{L\left(\text{target}\dfrac{\Delta_{\text{demand}}}{\Delta_{bb\_\text{calc}}}\right)}(\%)}{3.25\left(1-\dfrac{P}{A_g f_c'}\right)\left(1+\dfrac{L}{10D}\right)} - 1\right) \quad (13)$$

Fig. 9 shows the implications of using Eq. (13) to proportion the confinement reinforcement in a spiral-reinforced column. Fig. 9 was developed for a buckling probability of 10%, which corresponds to $\Delta_{\text{demand}}/\Delta_{bb\_\text{calc}} = 2/3$ (Fig. 7). The confinement requirements increase as drift ratio and axial load increase, and in some cases, the required confinement to prevent bar buckling exceeds the spiral requirements for earthquake-resistant construction (Eq. 21-2) of the American Concrete Institute Building Code Requirements for Structural Concrete (ACI 2002). Similar figures can be generated for other column types and target probabilities of buckling.

Conclusions

The assembled database made it possible to develop a procedure to estimate the likelihood of longitudinal bar buckling in flexure-dominant reinforced concrete columns based on imposed column deformation.

The coefficients of variation of the ratio of the measured displacement to the calculated displacement at the onset of bar buckling ($\Delta_{bb}/\Delta_{bb\_\text{calc}}$) were similar for the relationships based on plastic rotation, drift ratio, and displacement ductility. A modified version of the derived drift ratio relationship is proposed for earthquake-engineering applications.

$$\frac{\Delta_{bb\_\text{calc}}}{L}(\%) = 3.25\left(1 + k_{e\_bb}\rho_{\text{eff}}\frac{d_b}{D}\right)\left(1 - \frac{P}{A_g f_c'}\right)\left(1 + \frac{L}{10D}\right)$$
$$(14)$$

where $k_{e\_bb} = 40$ for rectangular-reinforced columns and 150 for spiral-reinforced columns; $\rho_{\text{eff}} = \rho_s f_{ys}/f_c'$, ρ_s = volumetric transverse reinforcement ratio; f_{ys} = yield stress of the transverse reinforcement; d_b = diameter of the longitudinal reinforcing steel; P = axial load, A_g = gross area of the cross section; f_c' = concrete compressive strength; L = distance from the column base to the point of contraflexure; and D = column depth. Because little data were available for large values of s/d_b, k_{e_bb} should be taken as 0.0 for columns in which s/d_b exceeds 6.

The mean value of $\Delta_{bb}/\Delta_{bb\_\text{calc}}$ obtained with Eq. (14) with the limit on s/d_b was 1.01 with a coefficient of variation of 25% for rectangular columns and 0.97 with a coefficient of variation of 24% for spiral-reinforced columns. The accuracy improves slightly if a more complex expression is used, but the increase in accuracy does not justify the increased complexity. By solving Eq. (14) for the effective confinement ratio, it is also possible to proportion the confinement reinforcement for new columns based on the column properties, the expected column deformation, and the target probability of bar buckling.

Acknowledgments

Notation

The following symbols are used in this paper:

A_g = gross area of column cross section;
$C_0, \ldots, C_4$ = parameters used in deformation approximations;
D = column depth;
d_b = bar diameter of longitudinal reinforcement;
E_s = elastic modulus of longitudinal reinforcement;
f_c' = compressive strength of concrete;
f_y = yield stress of longitudinal reinforcement;
f_{ys} = yield stress of transverse reinforcement;
G_0, G_1 = parameters used in approximation of normalized plastic curvature;
k_{e_bb} = transverse reinforcement coefficient;
L = distance from the column base to the point of contraflexure;
L_p = plastic hinge length;
P = column axial load;
α, β, ξ = parameters used in plastic hinge approximation;
Δ = total column displacement;
Δ_{bb} = column displacement at the onset of bar buckling;
Δ_{bb_calc} = calculated column displacement at the onset of bar buckling;
Δ_{demand} = expected column displacement demand;
Δ_p = plastic displacement of column;
Δ_y = yield displacement of column;
ε_{bb} = maximum compressive strain at the onset of bar buckling;
ε_n = maximum compressive strain in concrete;
ε_y = yield strain of the tension reinforcement;
$\eta_0, \ldots, \eta_2$ = parameters used in plastic curvature approximation;
θ_p = plastic rotation;
λ = parameter for yield curvature approximation;
ρ_{eff} = effective confinement ratio;
ρ_s = volumetric transverse reinforcement ratio;
θ_p = plastic curvature;
ϕ_{p_bb} = plastic curvature at the onset of longitudinal bar buckling;
ϕ_{p_n} = plastic curvature at maximum compressive strain ε_n;
ϕ_{p_norm} = normalized plastic curvature; and
χ_1, χ_1 = parameters used in buckling strain approximation.

References

American Concrete Institute (ACI). (2002). "Building code requirements for structural concrete." *ACI 318-02*, Detroit.

Atalay, M. B., and Penzien, J. (1975). "The seismic behavior of critical regions of reinforced concrete components as influenced by moment, shear and axial force." *Rep. No. EERC 75-19*, Univ. of California, Berkeley, Calif.

Bayrak, O. (1998). "Seismic performance of rectilinearly confined high strength concrete columns." Doctoral Dissertation, Dept. of Civil Engineering, Univ. of Toronto, Canada.

Bayrak, O., and Sheikh, S. (1996). "Confinement steel requirements for high strength concrete columns." *Proc., 11th World Conf. on Earthquake Engineering*, Aculpolco, Mexico, Paper No. 463.

Bayrak, O., and Sheikh, S. (2001). "Plastic hinge analysis." *J. Struct. Eng.*, 127(9), 1092–1100.

Berry, M. P. (2003). "Estimating flexural damage in reinforced concrete columns." Master's thesis, Dept. of Civil and Environmental Engineering, Univ. of Washington, Seattle.

Berry, M. P., and Eberhard, M. O. (2003). "Performance models for flexural damage in reinforced concrete columns." *Pacific Earthquake Engineering Research Center Report 2003*, Univ. of California, Berkeley, Calif.

Berry, M. P., and Eberhard, M. O. (2004) "PEER structural performance database user's manual." Pacific Earthquake Engineering Research Center Report 2004 ⟨www.ce.washington.edu/~peeral⟩, Univ. of California, Berkeley, Calif.

Bresler, B., and Gilbert, P. H. (1961). "Tie requirements for reinforced concrete columns." *ACI J.*, 58(5), 555–570.

Calderone, A. J., Lehman, D. E., and Moehle, J. P. (2000). "Behavior of reinforced concrete bridge columns having varying aspect ratios and varying lengths of confinement." *Pacific Earthquake Engineering Research Center Rep. 2000/08*, Univ. of California, Berkeley, Calif.

Cheok, G. S., and Stone, W. C. (1986). "Behavior of 1/6-scale model bridge columns subjected to cycle inelastic loading." *NBSIR 86-3494*, U.S. National Institute of Standards and Technology, Gaithersburg, Md.

Corley, W. G. (1966). "Rotational capacity of reinforced concrete beams." *J. Struct. Div. ASCE*, 92(5), 121–146.

Davey, B. E. (1975). "Reinforced concrete bridge piers under seismic loading." *Master of Engineering Report*, Civil Engineering Dept., Univ. of Canterbury, Christchurch, New Zealand.

Dhakal, R., and Maekawa, K. (2002). "Reinforcement stability and fracture of cover concrete in reinforced concrete members." *J. Struct. Eng.*, 128(10), 1253–1262.

Eberhard, M. O. (2000). "Consequences of bridge damage on functionality." *Proc., PEER Invitational Workshop on Performance-Based Engineering Concepts for Bridges*, Palo Alto, Calif.

Ghee, A. B., Priestley, M. J. N., and Park, R. (1981). "Ductility of reinforced concrete bridge piers under seismic loading." *Rep. 81-3*, Dept. of Civil Engineering, Univ. of Canterbury, Christchurch, New Zealand.

Gomes, A., and Appleton, J. (1997). "Nonlinear cyclic stress-strain relationship of reinforcing bars including buckling." *Eng. Struct.*, 19(10), 822–826.

Henry, L., and Mahin, S. A. (1999). "Study of buckling of longitudinal bars in reinforced concrete bridge columns." *Report to the California Dept. of Transportation*.

Hose, Y. D. (2001). "Seismic performance and failure behavior of plastic hinge regions in flexural bridge columns." PhD dissertation, Dept. of Structural Engineering, Univ. of California, San Diego.

Hose, Y. D., Seible, F., and Priestley, M. J. N. (1997). "Strategic relocation of plastic hinges in bridge columns." *Structural Systems Research Project, 97/05*, University of California, San Diego.

Kowalsky, M. J., Priestley, M. J. N., and Seible, F. (1999). "Shear and flexural behavior of lightweight concrete bridge columns in seismic regions." *ACI Struct. J.*, 96(1), 136–148.

Kunnath, S., El-Bahy, A., Taylor, A., and Stone, W. (1997). "Cumulative seismic damage of reinforced concrete bridge piers." *Technical Rep. NCEER-97-0006*, National Center for Earthquake Engineering Research, Buffalo, N.Y.

Lehman, D. E., Gookin, S. E., Nacamuli, A. M., and Moehle, J. P. (2001). "Repair of earthquake-damaged bridge columns." *ACI Struct. J.*, 98(2), 233–242.

Lehman, D. E., and Moehle, J. P. (2000). "Seismic performance of well-confined concrete bridge columns." *Pacific Earthquake Engineering*

Research Center Rep. 1998/01*, Univ. of California, Berkeley, Calif.

Mattock, A. H. (1967). "Discussion of 'Rotational capacity of reinforced concrete beams,' by W. G. Corley." *J. Struct. Div. ASCE*, 93(2), 519–522.

Monti, G., and Nuti, C. (1992). "Nonlinear cyclic behavior of reinforcing bars including buckling." *J. Struct. Eng.*, 118(12), 3268–3284.

Moyer, M., and Kowalsky, M. (2001). "Influence of tension strain on buckling of reinforcement in RC bridge columns." Dept. of Civil Engineering, North Carolina State Univ. , Raleigh, N.C.

Nelson, J. M. (2000). "Damage model calibration for reinforced concrete columns." Master's thesis, Dept. of Civil and Environmental Engineering, Univ. of Washington, Seattle.

Pantazopoulou, S. J. (1998). "Detailing for reinforcement stability in reinforced concrete members." *J. Struct. Eng.*, 124(6), 623–632.

Papia, M., and Russo, G. (1989). "Compressive concrete strain at buckling of longitudinal reinforcement." *J. Struct. Eng.*, 115(2), 382–397.

Park, R., and Paulay, T. (1990). "Use of interlocking spirals for transverse reinforcement in bridge columns." *Strength and ductility of concrete substructures of bridges*, *RRU (Road Research Unit) Bulletin 84*, 1, 77–92.

Priestley, M. J. N., and Park, R. (1987). "Strength and ductility of concrete bridge columns under seismic loading." *ACI Struct. J.*, 84(1), 61–76.

Priestley, M. J. N., Seible, F., and Calvi, G. M. (1996). *Seismic design and retrofit of bridges*, Wiley, New York.

Ranf, R. T., Nelson, J., Price, Z., Eberhard, M. O., and Stanton, J. F. (2003). "Accumulation of flexural damage in lightly reinforced concrete columns." *Pacific Earthquake Engineering Research Center Report PEER-2003*, Univ. of California, Berkeley, Calif.

Rodriguez, M., Botero, J., and Villa, J. (1999). "Cyclic stress-strain behavior of reinforcing steel including effect of buckling." *J. Struct. Eng.*, 125(6), 605–612.

Saatcioglu, M., and Baingo, D. (1999). "Circular high-strength concrete columns under simulated seismic loading." *J. Struct. Eng.*, 125(3), 272–280.

Saatcioglu, M., and Grira, M. (1999). "Confinement of reinforced concrete columns with welded reinforcement grids." *ACI Struct. J.*, 96(1), 29–39.

Saatcioglu, M., and Razvi, S. R. (1994). "Behavior of high strength columns subjected to axial load." *Proc., 5th National Conf. on Earthquake Engineering Research Inst.*, 2, Oakland, Calif.

Sawyer, H. A. (1964). "Design of concrete frames for two failure states." *Proc., Int. Symposium on the Flexural Mechanics of Reinforced Concrete*, ASCE-ACI, Miami, 405–431.

Scribner, C. F. (1986). "Reinforcement buckling in reinforced concrete flexural members." *ACI J.*, 83(6), 966–973.

Soesianawati, M. T., Park, R., and Priestley, M. J. N. (1986). "Limited ductility design of reinforced concrete columns." *Rep. 86-10*, Dept. of Civil Engineering, Univ. of Canterbury, Christchurch, New Zealand.

Stone, W. C., and Cheok, G. S. (1989). "Inelastic behavior of full-scale bridge columns subjected to cyclic loading." *NIST Building Science Series 166*, U.S. National Institute of Standards and Technology, Gaithersburg, Md.

Tanaka, H., and Park, R. (1990). "Effect of lateral confining reinforcement on the ductile behavior of reinforced concrete columns." *Rep. 90-2*, Dept. of Civil Engineering, Univ. of Canterbury, Christchurch, New Zealand.

Thomsen, J., and Wallace, J. (1994). "Lateral load behavior of reinforced concrete columns constructed using high-strength materials." *ACI Struct. J.*, 91(5), 605–615.

Vu, N. D., Priestley, M. J. N., Seible, F., and Benzoni, G. (1998). "Seismic response of well confined circular reinforced concrete columns with low aspect ratios." *Proc., 5th Caltrans Seismic Research Workshop*, Sacramento, Calif.

Watson, S. (1989). "Design of reinforced concrete frames of limited ductility." *Rep. 89-4*, Dept. of Civil Engineering, Univ. of Canterbury, Christchurch, New Zealand.

Wehbe, N., and Saiidi, M. S., and Sanders, D. (1998). "Confinement of

rectangular bridge columns for moderate seismic areas." *National Center for Earthquake Engineering Research (NCEER) Bulletin*, 12(1).

Wong, Y. L., Paulay, T., and Priestley, M. J. N. (1990). "Squat circular bridge piers under multi-directional seismic attack." *Rep. 90-4*, Dept. of Civil Engineering, Univ. of Canterbury, Christchurch, New Zealand.

Xiao, Y., and Martirossyan, A. (1998). "Seismic performance of high-strength concrete columns." *J. Struct. Eng.*, 124(3), 241–251.

Xiao, Y., and Yun, H. W. (2002). "Experimental studies on full-scale high-strength concrete columns." *ACI Struct. J.*, 99(2), 199–207.

Zahn, F. A., Park, R., and Priestley, M. J. N. (1986). "Design of reinforced bridge columns for strength and ductility."*Rep. 86-7*, Dept. of Civil Engineering, Univ. of Canterbury, Christchurch, New Zealand.